# Contra-lateral bone loss at the distal radius in postmenopausal women after a distal radius fracture

Bone 101 (2017) 245–251

Contents lists available at ScienceDirect

Bone

journal homepage: www.elsevier.com/locate/bone

Full Length Article

# Contra-lateral bone loss at the distal radius in postmenopausal women after a distal radius fracture: A two-year follow-up HRpQCT study

Joost J.A. de Jong [a,b,*], Jacobus J.C. Arts [c,d,e], Paul C. Willems [c,d], Sandrine P.G. Bours [b], Judith P.A. Bons [f], Paul P.C.A. Menheere [f], Bert van Rietbergen [e], Piet P. Geusens [b,c,g], Joop P.W. van den Bergh [a,b,g,h]

[a] NUTRIM School for Nutrition and Translational Research in Metabolism, Maastricht University Medical Center, The Netherlands
[b] Department of Rheumatology, Maastricht University Medical Center, The Netherlands
[c] CAPHRI School for Public Health and Primary Care, Maastricht University Medical Center, The Netherlands
[d] Department of Orthopaedic Surgery, Maastricht University Medical Center, The Netherlands
[e] Faculty of Biomedical Engineering, Section Orthopaedic Biomechanics, Eindhoven University of Technology, The Netherlands
[f] Central Diagnostic Laboratory, Maastricht University Medical Center, Maastricht, The Netherlands
[g] Faculty of Medicine and Life Sciences, Hasselt University, Belgium
[h] Department of Internal Medicine, VieCuri Medical Center Venlo, The Netherlands

ARTICLE INFO

*Article history:*
Received 16 November 2016
Revised 21 March 2017
Accepted 10 May 2017
Available online 11 May 2017

*Keywords:*
Injury/fracture healing
Osteoporosis
Biochemical markers of bone turnover
Bone QCT/μCT
Anti-resorptives

ABSTRACT

Opposite to the fracture side, bone mineral density (BMD) measured by DXA at the contra-lateral side does not change after a distal radius fracture. However, it is unknown if also bone micro-architecture and strength at the contralateral side are unaffected. Therefore, the aim of this study was to assess BMD, micro-architecture and bone mechanical properties at the contra-lateral side during two years follow-up after a distal radius fracture using high resolution peripheral quantitative computed tomography (HRpQCT). The contra-lateral distal radius of 15 postmenopausal women (mean age 64 ± 8 years) with a distal radius fracture treated by cast immobilization was scanned by HRpQCT at baseline, 3 months and 2 years post-fracture. BMD and cortical and trabecular micro-architecture were measured and biomechanical parameters were estimated using micro finite element analysis (μFEA). Additionally, markers of bone resorption and formation were measured at each visit. Bone parameters and turnover markers across the three visits were analysed using a linear mixed-effect model with Bonferroni correction. Two years post-fracture, a significant decrease from baseline was found in cortical BMD (−4.2%, $p < 0.001$), failure load (−6.1%, $p = 0.001$), stiffness in compression (−5.7%, $p = 0.003$) and bending (−6.4%, $p = 0.008$), and bone formation (−47.6%, $p = 0.010$). No significant changes from baseline were observed in total and trabecular BMD, nor in cortical or trabecular micro-architecture and neither in bone resorption. Results were similar between patients with or without adequate anti-osteoporosis drug treatment. We found a significant decline in BMD in the cortical but not the trabecular region, and a reduction in bone strength and stiffness at the contra-lateral side two years after a distal radius fracture. These changes exceeded the changes that may be expected due to aging, even in the presence of adequate anti-osteoporosis treatment.



## 1. Introduction

After fracture of a lower extremity, bone loss often occurs at the fracture side, even at locations more distant from the fracture, due to a period of consequent absence of weight-bearing and immobilization [1,2]. Bone loss has also been observed at the contra-lateral side after a hip fracture up to two year post-fracture [3–6] (but not after a tibial shaft fracture [2]).

Following Wolff's law, which states that a bone's internal structure and shape adapt itself to the mechanical loading conditions imposed on it [7], it is not surprising that the bone at the contra-lateral hip is resorbed after a period of decreased loading due to bed-rest or immobilization. This effect is therefore not expected at non-weight-bearing limbs, such as the forearm, for which the contra-lateral side is not immobilized. Indeed, several studies reported no changes in BMD at the contra-lateral radius one year after a Colles' fracture [8,9].

Whereas the aforementioned studies only took areal bone mineral density (aBMD) assessed by dual-energy x-ray absorptiometry (DXA) into account, we recently used high resolution peripheral quantitative computed tomography in combination with micro finite element analysis (μFEA) to assess changes in volumetric bone mineral density (vBMD), bone micro-architecture and bone strength during the healing process of distal radius fractures [10,11]. In this study, large changes in vBMD, micro-architecture and biomechanical parameters were found at the

* Corresponding author at: Maastricht University Medical Center, Department of Rheumatology, P.O. Box 5800, 6202 AZ Maastricht, The Netherlands.
*E-mail address:* joost.dejong@maastrichtuniversity.nl (J.J.A. de Jong).

http://dx.doi.org/10.1016/j.bone.2017.05.011
8756-3282/

fracture side during a follow-up of two years post-fracture. Also, we found no changes in these bone parameters at the contra-lateral side during the first 3 months post-fracture [10], but it is unknown if the bone parameters remain unchanged during a longer time post-fracture.

Since earlier studies found no changes in aBMD at the contra-lateral side after a forearm fracture [8,9], we hypothesized that after the initial 3-month period of no change, no changes in vBMD and therefore also not in micro-architecture and bone strength occurs at the contra-lateral side during the two years post-fracture. To address these hypotheses, we monitored vBMD, micro-architecture and bone biomechanical properties at the contra-lateral radius using HRpQCT and μFEA during a period of two years after a distal radius fracture.

## 2. Methods

### 2.1. Subjects

The patients in this study all participated in a medical ethical approved clinical trial on fracture healing (registration no. NTR3821) [11]. Besides the initial inclusion and exclusion criteria (Table 1), an additional exclusion criterion for the current study was a previous fracture at the contra-lateral side. All patients were informed and gave written informed consent prior to participation.

### 2.2. HRpQCT scanning

HRpQCT (XtremeCT, Scanco, Brüttisielen Switzerland) scans of the contra-lateral forearm were performed at baseline (one to two weeks post-fracture) and three months and two years post-fracture. The scans were made at standard clinical high resolution settings, i.e. with a tube voltage of 60 kVp, tube current of 900 μA and a 100 ms integration time. All scans were reconstructed using an isotropic voxel size of 82 μm. At baseline and the first follow-up visit, the region of interest (ROI) incorporated a 9 mm long section starting 9.5 mm proximal of the os lunate bone in all patients. Due to changes in the study protocol, the ROI at the two-year follow-up visit was extended to a 18 mm long section. The start of this section differed between patients such that it matched the scanned region at fracture side [11].

To prevent motion artefacts, the forearm of each patient was fixed in a cylindrical carbon holder (XCT Carpal, Pearltec AG, Switzerland) with an inflatable cushion as described previously [12]. After scanning, all HRpQCT images were checked for motion-induced image artefacts and were quality graded according to the manufacturer's guidelines and as described by Pialat et al. [13] In case of insufficient quality, i.e. grade four and five, the scan was repeated once.

Quality control during the study period was assured by regular HRpQCT measurements of a calibration phantom containing rods of different densities (0, 100, 200, 400, and 800 mgHA/cm$^3$).

### 2.3. Evaluation of bone density and micro-architecture

Since the scanned region at the last visit differed from the first two visits, the common ROI was based on matching the first and last slices of the baseline and three-month scans to the corresponding slices at the two-year scan (Fig. 1).

The bone density and micro-architectural parameters within this common ROI were then evaluated using the standard patient evaluation protocol provided by the manufacturer (Scanco Medical AG) as described earlier [14]. In short, after semi-automatically deriving the periosteal contour the total region was divided in a cortical and trabecular region and each region was segmented and combined to into a 3D model to represent the micro-architecture. vBMD [mgHA/cm$^3$] was calculated in the total (Dtot), trabecular (Dtrab) and cortical (Dcort) region. Furthermore, trabecular number (Tb.N) [mm$^{-1}$], thickness (Tb.Th) [mm] and separation (Tb.Sp) [mm] were determined to assess the trabecular micro-architecture, and cortical thickness (Ct.Th) [mm] and perimeter (Ct.Pm) [mm] were assessed for the cortical compartment. In addition to the standard patient evaluation protocol, extended cortical analysis as described by Burghardt et al. [15] was performed to assess cortical porosity (Ct.Po) [%], cortical pore volume (Ct.Po.V) [mm$^3$] and diameter (Ct.Po.V) [mm].

### 2.4. Finite element analysis

To assess the bone's mechanical properties, micro finite element (μFE) models were created directly from the segmented HRpQCT images similar to earlier studies [16,17]. In short, to obtain a representative μFE model of the bone's micro-architecture each voxel in the segmented images that represents bone tissue was converted into a brick element of the same size. These μFE models typically consisted of around 1 million elements. Constant material properties were assigned to each element, i.e. a Young's modulus of 10 GPa and a Poisson's ratio of 0.3.

Next, a compression load was simulated by applying a 'high friction' compression test with a prescribed displacement in the axial direction of 1% of the total length, from which the compression stiffness (Scomp) [kN/mm] and ultimate failure load (F.Ult) [kN] were estimated.

Additionally, by applying representative loading scenarios also torsional (Stors) [kN mm/rad] and bending stiffness (Sbend) [kN mm$^2$] were estimated in a similar way as in our previous study and which has been described earlier [10].

### 2.5. DXA and biochemical analyses

In accordance with Dutch standard care when a patient over the age of 50 years comes to clinic with a fracture, all patients in this study visited the fracture liaison service (FLS) between four and eight weeks post-fracture for assessment of osteoporosis and vertebral fractures by DXA(Hologic Discovery A; Hologic Inc., Waltham, MA). If the patients

**Table 1**
Inclusion and exclusion criteria.

| Inclusion criteria | Exclusion criteria |
|---|---|
| • Postmenopausal women<br>• Older than 50 years<br>• Stable distal radius fracture<br>• Treated by cast immobilization<br>• Willing and able to participate | • Previous fracture at the same or contra-lateral location<br>• Active or suspected infection<br>• Malignant disease in the past 12 months<br>• Neuromuscular or neurosensory deficit which would limit the ability to assess performance<br>• Known systemic or metabolic disorders leading to progressive bone deterioration<br>• Active inflammatory disease<br>• Use of oral glucocorticoids<br>• Mental incompetence<br>• Severe concurrent joint involvements<br>• Selection for other trial on distal radius fractures |

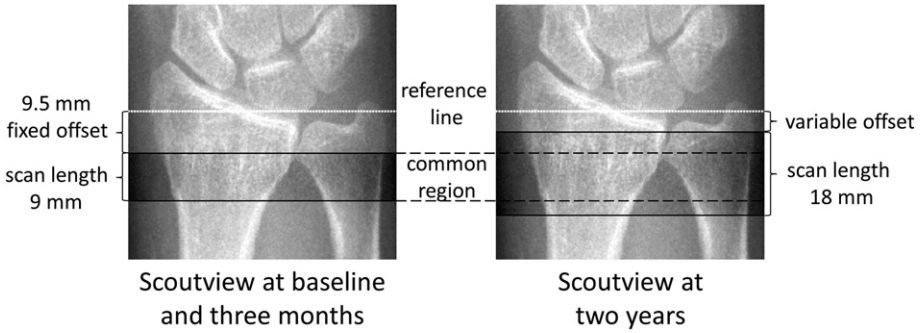


**Fig. 1.** Scoutview showing the scanned regions at baseline and three months (left) and two years (right). The common region between the three scans is marked within the dotted lines, and is used for the assessment of bone density, micro-architecture and biomechanical parameters.

already had a DXA scan in the last year prior to the fracture, this previous DXA measurement was used.

Additionally, blood serum samples were taken for biochemical analyses that included calcium (Photometric assay; Roche Diagnostics, Basel, Switzerland), 25-hydroxy-vitamin D (chemiluminescence immunoassay; IDS-iSYS Immunodiagnostic Systems GmbH, Frankfurt, Germany), parathyroid hormone (chemiluminescence immunoassay; Siemens, Erlangen, Germany), thyroid-stimulating hormone (electrochemiluminescence immunoassay; Roche Diagnostics, Basel, Switzerland) and free thyroxine (fluorescence immunoassay; Perkin Elmer, Turku, Finland) for diagnosis of hyperthyroidism, hypercalcemia and hyperparathyroidism, which are known contributors to bone loss [18]. Furthermore, patients were asked about their current medication. If patients were diagnosed with osteoporosis, adequate anti-osteoporosis treatment was started by bisphosphonates, denosumab, calcium or vitamin-D, or a combination of these medications. At the end of the study, a telephone interview was conducted with each patient to check whether the patients were compliant to their treatment.

### 2.6. Serum markers of bone turnover

In addition to the standard biochemical analyses, venous blood samples were collected at each visit by puncture of the antecubital vein for assessment of bone turnover markers. Serum was separated from the blood clot within 20 min and freezed to −20 °C until analysis. Serum bone markers representing bone resorption (carboxy-terminal telopeptide of type I collagen (ICTP)) and bone formation (procollagen type-I N-terminal propeptide (PINP)) were assessed by radioimmunoassay (UniQ® PINP/ICTP; Orion Diagnostics, Espoo, Finland) in a certified laboratory. The calculated precision profile indicates a coefficient of variation below 10% over the range of 2.5 to 25 [μg/l] for ICTP and over the range of 25 to 140 [μg/l] for PINP. The observed LOB's (lower limit of blank) was 0.6 [μg/l] for ICTP and 2 [μg/l] for PINP.

### 2.7. Statistics

Patient's demographic and clinical baseline characteristics were reported in means and their standard deviations. HRpQCT derived bone parameters and the bone turnover markers at each visit were reported as estimated marginal means and their 95% confidence intervals which were obtained from a linear mixed effect model with visit as fixed effect and a compound symmetry covariance structure. The same linear mixed-effect model with Bonferroni correction was used to compare the bone parameters and bone turnover markers between the three visits.

A level of significance of 0.05 was used in all statistical analyses, and all analyses were performed with SPSS Statistics for Windows version 20.0 (IBM Corp., Armonk, USA).

## 3. Results

Fifteen patients were included in the study. The demographic and clinical baseline characteristics of these patients are presented in Table 2. At baseline, seven patients were already receiving calcium and/or vitamin D supplementation, and three of them were also being treated with alendronate. At three months post-fracture, anti-osteoporosis treatment was started (or continued) at the FLS: calcium and/or vitamin D supplementation started (or continued) in all patients. Additionally, seven patients started and three patients continued with alendronate 70 mg per week, and one patient started with subcutaneous injections of 60 mg denosumab every six months. The end-of-study telephone interview with each patient confirmed that the denosumab injections were administered correctly, and that compliance with alendronate treatment was 67%. One patient could not be contacted.

From the in total 45 HRpQCT measurements, nine measurements (20.0%, three at each visit) were of insufficient quality, due to motion artefacts. The average common ROI between the HRpQCT scans at the three visits consisted of 100.7 slices (91.5%).

### 3.1. Changes in bone density

In Table 3, the HRpQCT derived bone parameters as well as the percentage change from baseline at each visit within the common ROI are presented. During two years post-fracture, no significant changes

**Table 2**
Patients' demographic and clinical baseline characteristics (n = 15). If applicable, reference values are reported between parentheses.

| Characteristic | Mean (SD) |
|---|---|
| Age [years] | 63.7 (8.1) |
| DXA T-score at lumbar spine[a] | −2.3 (1.5) |
| Normal BMD [n; %] | 1 (7.1%) |
| Osteopenic [n; %] | 6 (42.9%) |
| Osteoporotic [n; %] | 7 (50.0%) |
| Presence of VF [n; %][b] | 5 (38.5%) |
| 25(OH)D [nmol/L] (15–162) | 66.5 (28.8) |
| 25(OH)D < 50 nmol/L [n;%] | 5 (33.3%) |
| 25(OH)D < 75 nmol/L [n;%] | 8 (53.3%) |
| Calcium [mmol/L] (2.10–2.55) | 2.44 (0.13) |
| PTH [pmol/L] (1.2–7.1) | 3.84 (1.95) |
| TSH [mU/L][c] (0.4–4.3) | 2.1 (0.7–18.8) |
| Hypercalcemia [n; %] | 0 (0.0%) |
| Hyperthyroidism [n; %] | 0 (0.0%) |
| Hyperparathyroidism [n; %] | 0 (0.0%) |

Values are reported as means and their standard deviations (SD) unless stated otherwise.
Abbreviations: DXA: dual-energy X-ray absorptiometry; BMD: bone mineral density; VF: vertebral fracture; 25(OH)D: 25-hydroxy-vitamin D; PTH: parathyroid hormone; TSH: thyroid-stimulating hormone.
[a] From one patient no DXA data was available.
[b] VFA not performed in two patients.
[c] Not normally distributed. Median and range are reported.

**Table 3**
Estimated marginal means (EMM) and 95% confidence intervals (95%CI) of the BMD, micro-architectural and biomechanical parameters at the contra-lateral side and markers of bone formation and resorption at each study visit.

| Parameter | EMM (95%CI) at baseline | EMM (95%CI) at 3 months | Change from baseline (%) | p-Value | EMM (95%CI) at 2 years | Change from baseline (%) | p-Value |
|---|---|---|---|---|---|---|---|
| vBMD | | | | | | | |
| Dtot [mgHA/cm$^3$] | 251,4 (205,5–297,3) | 252,6 (206,8–298,5) | 0,51 | 1000 | 248,5 (202,6–294,3) | −1.16 | 1000 |
| Dtrab [mgHA/cm$^3$] | 104,8 (81,7–127,9) | 103,5 (80,4–126,6) | -1,28 | 1000 | 101,8 (78,7–124,9) | −2.86 | 0,800 |
| Dcort [mgHA/cm$^3$] | 798,6 (750,9–846,3) | 799,2 (751,5–846,9) | 0,07 | 1000 | 764,9 (717,1–812,6) | −4.23 | <0.001 |
| Micro-architecture | | | | | | | |
| Tb.N [mm$^{-1}$] | 1,5 (1,27–1,73) | 1,55 (1,32–1,79) | 3,74 | 0,627 | 1,56 (1,32–1,79) | 3,84 | 0,593 |
| Tb.Th [mm] | 0,056 (0,051–0,062) | 0,054 (0,049–0,060) | −3.49 | 0,524 | 0,053 (0,047–0,059) | −5.44 | 0,121 |
| Tb.Sp [mm] | 0,691 (0,517–0,865) | 0,666 (0,492–0,839) | −3.71 | 0,693 | 0,652 (0,479–0,826) | −5.61 | 0,231 |
| Ct.Th [mm] | 0,64 (0,51–0,77) | 0,65 (0,53–0,78) | 2,17 | 0,338 | 0,63 (0,51–0,76) | −1.03 | 1000 |
| Ct.Pm [mm] | 70,3 (66,6–73,9) | 70,3 (66,7–74,0) | 0,12 | 1000 | 70,7 (67,1–74,3) | 0,66 | 0,357 |
| Ct.Po[a] [%] | 2,78 (1,99–3,56) | 2,66 (1,87–3,45) | −4.14 | 1000 | 2,87 (2,08–3,66) | 3,43 | 1000 |
| Ct.Po.D[a] [mm] | 0,171 (0,159–0,184) | 0,174 (0,162–0,187) | 1,80 | 1000 | 0,17 (0,158–0,182) | −0.7 | 1000 |
| Ct.Po.V[a] [mm$^3$] | 10,1 (7,6–12,6) | 9,9 (7,5–12,4) | −1.60 | 1000 | 10,7 (8,2–13,1) | 5,46 | 1000 |
| Biomechanical | | | | | | | |
| F.Ult [kN] | 3,07 (2,64–3,51) | 3,06 (2,63–3,50) | −0.39 | 1000 | 2,89 (2,45–3,32) | −6.1 | 0,001 |
| Scomp [kN/mm] | 70,7 (59,6–81,8) | 70,5 (59,4–81,5) | −0.32 | 1000 | 66,7 (55,6–77,7) | −5.71 | 0,003 |
| Stors [kN mm/rad] | 1477 (1228–1727) | 1515 (1265–1764) | 2,53 | 1000 | 1435 (1186–1685) | −2.85 | 0,929 |
| Sbend [kN/mm$^2$] | 2647 (2202–3093) | 2667 (2221 − 3113) | 0,74 | 1000 | 2477 (2032–2923) | −6.42 | 0,008 |
| Bone turnover markers | | | | | | | |
| PINP [μg/L] | 54,5 (41,8–67,1) | 62,3 (50,1–74,5) | 14,33 | 0,963 | 28,5 (15,5–41,6) | −47,64 | 0,010 |
| ICTP [μg/L] | 3,7 (3,0–4,4) | 4 (3,3–4,6) | 6,58 | 1000 | 3,4 (2,7–4,1) | −7.64 | 1000 |

p-Values are obtained from a linear mixed-effect model.
Abbreviations: vBMD: volumetric bone mineral density; Dtot: total density; Dtrab: trabecular density; Dcort: cortical density; Tb.N: trabecular number; Tb.Th: trabecular thickness; Tb.Sp: trabecular separation; Ct.Th: cortical thickness; Ct.Pm: cortical perimeter; Ct.Po: cortical porosity; Ct.Po.D cortical pore diameter; Ct.Po·V cortical pore volume; F.Ult: ultimate failure load; Scomp: compression stiffness; Stors: torsional stiffness; Sbend: bending stiffness; PINP: procollagen type-I N-terminal propeptide; ICTP: carboxy-terminal telopeptide of type I collagen.
[a] Parameters are obtained using the extended cortical evaluation script.

occurred in total or trabecular vBMD. For cortical vBMD an initial 12 week period without change was followed by a decline that led to a change from baseline of −4.2% ($p < 0.001$) at two years post-fracture. Separate analysis of the two-year changes in cortical vBMD in the patients who were compliant with anti-resorptive treatment, i.e. alendronate or denosumab, that started three months post-fracture ($n = 5$) and the patients who did not receive or were not compliant with anti-resorptive treatment ($n = 7$), showed similar decreasing trends in cortical BMD (Fig. 2, left panel).

### 3.2. Changes in cortical and trabecular micro-architecture

No significant changes were observed in the trabecular and cortical micro-architectural parameters at the contra-lateral side during two years post-fracture.

### 3.3. Changes in bone mechanical properties

Similar to cortical BMD, also in compressive failure load (F.Ult) as well as stiffness in compression (Scomp) and bending (Sbend) an initial 12 week period without change was followed by a decline, which led to a change from baseline at two-years post-fracture of −6.1% ($p = 0.001$), −5.7% ($p = 0.003$) and −6.4% ($p = 0.008$), respectively. Torsional stiffness showed a comparable pattern, but the −2.9% change from baseline at two years post-fracture was not significant ($p = 0.929$). Separate analysis of the two-year changes in the patients who were compliant with anti-resorptive treatment, i.e. alendronate or denosumab, that started three months post-fracture ($n = 5$) and the patients who did not receive or were not compliant with anti-resorptive treatment ($n = 7$), showed a decreasing Scomp in patients who did not receive or were not compliant with alendronate treatment and in the patient treated with denosumab (Fig. 2, right panel), while Scomp tended to decrease less in the patients who were compliant with alendronate treatment that was started at three months post-fracture.

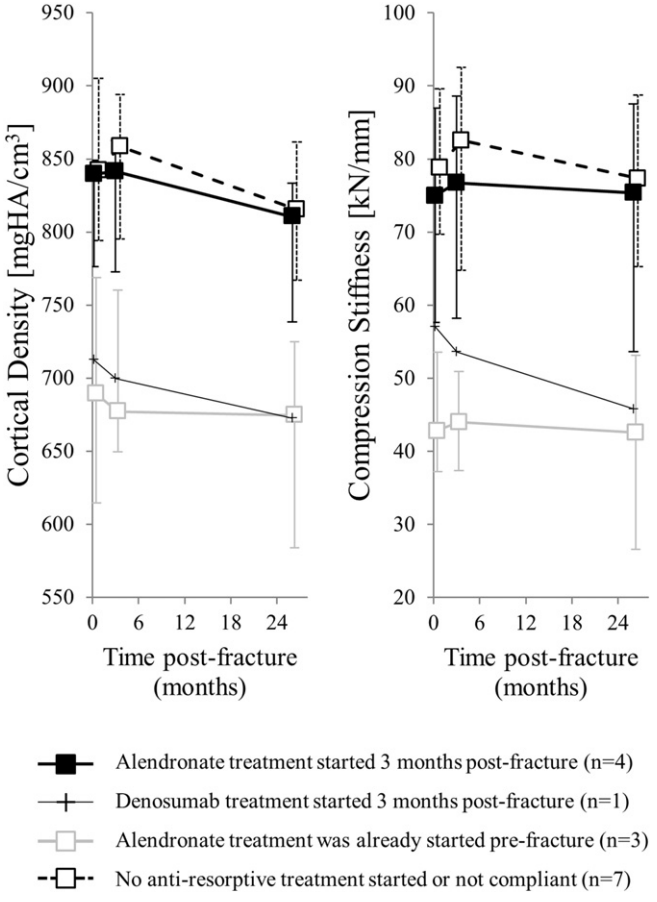


**Fig. 2.** Median and 25% and 75% percentiles of cortical density (left) and compression stiffness (right) at the contra-lateral radius at baseline, three months and two years after a fracture in patients who started with alendronate (dark thick straight line) or denosumab (dark thin straight line) treatment at three months post-fracture, patients who were already started with alendronate treatment pre-fracture (light straight line), and patients who did not start or were not compliant to anti-resorptive treatment (dotted line).

### 3.4. Changes in markers of bone formation and resorption

Markers of bone formation (PINP) and resorption (ICTP) as well as the percentage change from baseline at each visit are presented in Table 3. During the first three months post-fracture, no significant changes were observed in both markers. At two years post-fracture, a significant decrease from baseline was observed in PINP (−47.6%, p = 0.010), but not in ICTP (−7.6%, p = 1.000). A similar pattern was observed in patients who were compliant to alendronate treatment started at three months post-fracture and in patients who were not compliant or were not treated with alendronate. The patient who was treated with denosumab injections showed a clear decrease in levels of both PINP and ICTP (Fig. 3).

## 4. Discussion

This study showed a significant decrease of cortical vBMD and bone strength and stiffness at the contra-lateral distal radius two years after a stable distal radius fracture.

To our knowledge, there are only a few longitudinal studies that looked into bone changes at the contra-lateral side after a distal radius fracture. In these studies, no changes were observed in aBMD measured by DXA at the contra-lateral side [8,9], and thus our finding that we did not observe a change in total vBMD is consistent with current literature. With HRpQCT, however, it was possible to divide the total region in a cortical and trabecular compartment and analyse these compartments separately. We then found a decrease in cortical, but not in trabecular density. Also we did not find changes in cortical or trabecular micro-architecture.

The finding that trabecular density and micro-architecture remained constant during our two-year follow-up period is mainly consistent with current literature. Results from Burghart et al. [19] and Cheung et al. [20] showed that no changes are expected in trabecular density and micro-architectural parameters at the distal radius of untreated subjects (n = 13 and n = 74, respectively). Also Kawalilak et al. [21] found no changes in trabecular density at the distal radius of untreated subjects (n = 31), but did find a one-year decrease in trabecular number and increase trabecular thickness, indicating a shift towards a trabecular network with less but thicker trabeculae during this period. The reason for these different findings regarding trabecular micro-architecture remains unclear and should be further investigated.

Compared to literature, the two-year decline of 4.2% in cortical vBMD and >6.0% in the biomechanical parameters at the contra-lateral side after a forearm fracture appeared to be higher than expected during normal aging. A recent prospective HRpQCT study on age- and gender-related changes in vBMD, micro-architecture and bone strength found an annual change in cortical vBMD and failure load of −0.4% and −0.9%, respectively, in the group consisting of post-menopausal women (n = 51) [22]. The control group (n = 73) in a large HRpQCT intervention study on the effect of odanacatib showed a two-year decrease in cortical vBMD and estimated bone strength, of −1.65% and −1.61%, respectively [20]. Also the control group (n = 82) in another large HRpQCT intervention study on the effect of alendronate and denosumab showed a one-year decrease in cortical BMD of −1.5% [23], and in a small randomized controlled HRpQCT study on the effect of alendronate [19], cortical vBMD tended to decrease and estimated failure load and stiffness in compression significantly decreased with approximately 3% in the control group (n = 13) during the two-year follow-up. Therefore, the results in our study suggest that there is a higher rate of bone loss in the cortical region in post-menopausal women with a distal radius fracture. Interestingly, a higher than expected decline in BMD was also observed after hip fractures by Magaziner et al. [4,5]. After hip fractures, the contra-lateral side is often immobilized as well due to a period of bedrest, which could attribute to the higher decline. However, this is not the case for fore-arm fractures and one could even argue that the non-fractured fore-arm is used more than in the pre-fracture situation.

The greater than expected declines in cortical vBMD and bone strength are particularly surprising, since it has been shown that alendronate and, to a larger extent, denosumab increase BMD by decreasing bone resorption, and secondary also bone formation [19,23–25]. However, in two studies patients with a fracture after age 50 were excluded [19,23].

Whereas levels of bone turnover markers decreased in the patient being treated with denosumab, levels of bone resorption marker ICTP

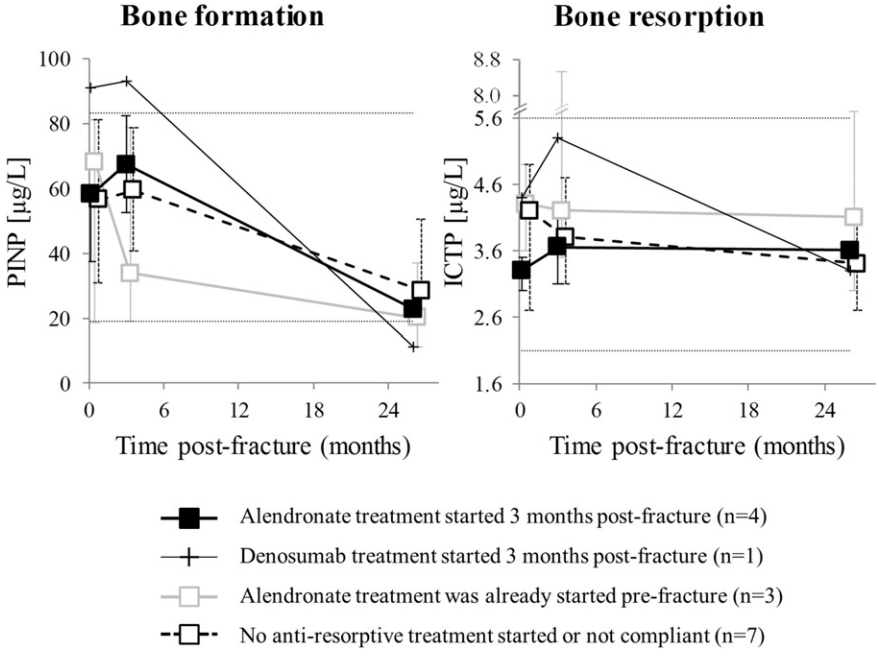


**Fig. 3.** Median and 25% and 75% percentiles of bone formation and resorption markers at baseline, three months and two years post-fracture for patients who started with alendronate (dark thick straight line) or denosumab (dark thin straight line) treatment at three months post-fracture, patients who were already started with alendronate treatment pre-fracture (light straight line), and patients who did not start or were not compliant to anti-resorptive treatment (dotted line). The thin dotted lines mark the lower and upper reference limits as reported by the manufacturer from the analysis kits.

remained unchanged and levels of bone formation marker PINP decreased by almost 50% in patients with or without alendronate treatment. This could indicate uncoupling of bone resorption and formation in these patients, which is in line with the observed loss in cortical vBMD. The results of the bone turnover markers, however, should be interpreted in the context of fracture healing. Whereas the decreased bone formation is compatible with healing, i.e. the initial increase in PINP due to callus formation has decreased to low-normal at two years post-fracture, the unchanged bone resorption is difficult to explain. Still, non-compliance can be an issue [26] for alendronate, but not for denosumab. Other explanations include persistent bone resorption of the callus, or another underlying yet unidentified metabolic bone disorder, associated with a recent fracture. Further elucidation of this process needs to be addressed in future studies.

Given the precision error of the technique to assess cortical vBMD is approximately 1% [14,27,28], individual changes in cortical BMD need to exceed the least significant change (LSC) of ±2.77% to be considered true changes. Since the two-year decline in cortical vBMD in all but one subject was larger than the LSC, we can indeed conclude that cortical vBMD truly decreased. The precision of the technique to assess the biomechanical parameters, however, is slightly lower with 3.6% [28], and hence the LSC for the biomechanical parameters is ±10%. A two-year decline in compression stiffness larger than 10% was observed in only four subjects, and in the remaining eleven subjects the two-year decline in compression stiffness could not be considered true change. On a group level, however, the two-year decline in the biomechanical parameters is still significant.

The finding that the decrease in cortical density was accompanied by a decrease in the biomechanical parameters is not surprising, given the fact that the cortex carries a large proportion of the loads at the distal radius [29,30]. Although also intra-cortical porosity is a good predictor for bone strength [31–33], no significant changes in cortical porosity were found in our study. However, this might be a limitation of the resolution of the currently used HRpQCT device, which is not sufficient to capture small pores. Additionally, the precision of the currently used HRpQCT devices to assess cortical porosity is rather poor, i.e. RMS-CV% of >10% [15,28,34]. Future research on cortical porosity after a fracture should, therefore, make use of the second generation HRpQCT scanners, which have a higher spatial resolution.

### 4.1. Limitations

Our study has several limitations that are noteworthy. First of all, due to the exploratory nature of this pilot study a small number of subjects were included and in combination with exclusion of measurements of insufficient quality, hence, we were limited in our statistical analyses. Also, we were not able to include a control group so it was not possible to make a comparison with subjects that did not fracture their wrist. Third, although not the purpose of this study, we did not longitudinally monitor vBMD at other sites than the distal radius, e.g. QCT of the lumbar spine, hip or tibia, which could have provided more insight into the cortical bone loss. A large cross-sectional study by Riggs et al. [35] showed that cortical vBMD loss occurred at the distal radius and tibia was age-related, whereas this was not the case for cortical vBMD loss at the femoral neck. At the lumbar spine, where little cortical bone is present, trabecular vBMD loss was also age-related. Whether these relations are affected by the occurrence of a distal radius fracture remains unknown. Additional analyses, however, did not reveal clear indications for different patterns of cortical vBMD and strength loss between patients with and without vertebral fractures in our study (data not shown). Fourth, we could not perform HRpQCT measurements between three months and two years post-fracture due to the time passed before we received approval from our ethical committee for an extension on the initial research protocol, in which a follow-up up to 3 months post-fracture was approved. Last, due to a change in the study protocol the HRpQCT scans at the two-year visit consisted of two consecutive stacks of 110 slices each. As a result of patient motion during scanning, these stacks might not be aligned perfectly which could lead to an underestimation of bone strength and stiffness. However, we discarded the measurements of insufficient quality in our linear mixed-effect model and therefore the shift between stacks should be minimal, thus leaving less room for errors. Moreover, not discarding the measurements of insufficient quality led to the same conclusions (data not shown).

## 5. Conclusion

We conclude that in post-menopausal women a stable fracture at the distal radius is associated with accelerated cortical bone loss and concomitant reduction of bone strength but not with micro-architectural changes at the contra-lateral distal radius, even in the presence of adequate anti-resorptive treatment.

## Disclosures

This study was supported by a grant from the Weijerhorst Foundation (WH-2).

B. van Rietbergen is a consultant for Scanco Medical AG.

J.J. Arts is a board member of workgroup Biotechnology of the Dutch Orthopedic Association (NOV) and board member Dutch Society for Biomaterials and Tissue Engineering.

P.C. Willems is a board member of the Dutch Spine Society (association of spine surgeons).

## Acknowledgements

The Authors would like to thank Frans Heyer for collection of the venous blood samples.

## References

[1] Clement E. van der Poest, M. van Engeland, H. Ader, J.C. Roos, P. Patka, P. Lips, Alendronate in the prevention of bone loss after a fracture of the lower leg, J. Bone Miner. Res. 17 (2002) 2247–2255.
[2] S.W. Veitch, S.C. Findlay, A.J. Hamer, A. Blumsohn, R. Eastell, B.M. Ingle, Changes in bone mass and bone turnover following tibial shaft fracture, Osteoporos. Int. 17 (2006) 364–372.
[3] K.M. Fox, J. Magaziner, W.G. Hawkes, J. Yu-Yahiro, J.R. Hebel, S.I. Zimmerman, L. Holder, R. Michael, Loss of bone density and lean body mass after hip fracture, Osteoporos. Int. 11 (2000) 31–35.
[4] L. Reider, T.J. Beck, M.C. Hochberg, W.G. Hawkes, D. Orwig, J.A. YuYahiro, J.R. Hebel, J. Magaziner, Study of Osteoporotic Fractures Research G, Women with hip fracture experience greater loss of geometric strength in the contralateral hip during the year following fracture than age-matched controls, Osteoporos. Int. 21 (2010) 741–750.
[5] J. Magaziner, L. Wehren, W.G. Hawkes, D. Orwig, J.R. Hebel, L. Fredman, K. Stone, S. Zimmerman, M.C. Hochberg, Women with hip fracture have a greater rate of decline in bone mineral density than expected: Another significant consequence of a common geriatric problem, Osteoporos. Int. 17 (2006) 971–977.
[6] M. Karlsson, J.A. Nilsson, I. Sernbo, I. Redlund-Johnell, O. Johnell, K.J. Obrant, Changes of bone mineral mass and soft tissue composition after hip fracture, Bone 18 (1996) 19–22.
[7] J. Wolff, Das Gesetz der Transformation der Knochen. Verlag von August Hirschwald, 1892.
[8] Clement E. van der Poest, P. Patka, K. Vandormael, H. Haarman, P. Lips, The effect of alendronate on bone mass after distal forearm fracture, J. Bone Miner. Res. 15 (2000) 586–593.
[9] B.M. Ingle, S.M. Hay, H.M. Bottjer, R. Eastell, Changes in bone mass and bone turnover following distal forearm fracture, Osteoporos. Int. 10 (1999) 399–407.
[10] J.J. de Jong, P.C. Willems, J.J. Arts, S.G. Bours, P.R. Brink, T.A. van Geel, M. Poeze, P.P. Geusens, B. van Rietbergen, J.P. van den Bergh, Assessment of the healing process in distal radius fractures by high resolution peripheral quantitative computed tomography, Bone 64C (2014) 65–74.
[11] J.J. de Jong, F.L. Heyer, J.J. Arts, M. Poeze, A.P. Keszei, P.C. Willems, B. van Rietbergen, P.P. Geusens, J.P. van den Bergh, Fracture repair in the distal radius in post-menopausal women: A follow-up two years post-fracture using HRpQCT, J. Bone Miner. Res. (2015).
[12] J.J. de Jong, J.J. Arts, U. Meyer, P.C. Willems, P.P. Geusens, J.P. van den Bergh, B. van Rietbergen, Effect of a cast on short-term reproducibility and bone parameters obtained from HR-pQCT measurements at the distal end of the radius, J. Bone Joint Surg. Am. 98 (2016) 356–362.
[13] J.B. Pialat, A.J. Burghardt, M. Sode, T.M. Link, S. Majumdar, Visual grading of motion induced image degradation in high resolution peripheral computed tomography:

impact of image quality on measures of bone density and micro-architecture, Bone 50 (2012) 111–118.
[14] S. Boutroy, M.L. Bouxsein, F. Munoz, P.D. Delmas, In vivo assessment of trabecular bone microarchitecture by high-resolution peripheral quantitative computed tomography, J. Clin. Endocrinol. Metab. 90 (2005) 6508–6515.
[15] A.J. Burghardt, H.R. Buie, A. Laib, S. Majumdar, S.K. Boyd, Reproducibility of direct quantitative measures of cortical bone microarchitecture of the distal radius and tibia by HR-pQCT, Bone 47 (2010) 519–528.
[16] W. Pistoia, B. van Rietbergen, E.M. Lochmuller, C.A. Lill, F. Eckstein, P. Ruegsegger, Estimation of distal radius failure load with micro-finite element analysis models based on three-dimensional peripheral quantitative computed tomography images, Bone 30 (2002) 842–848.
[17] N. Dalzell, S. Kaptoge, N. Morris, A. Berthier, B. Koller, L. Braak, B. van Rietbergen, J. Reeve, Bone micro-architecture and determinants of strength in the radius and tibia: age-related changes in a population-based study of normal adults measured with high-resolution pQCT, Osteoporos. Int. 20 (2009) 1683–1694.
[18] S.P. Bours, J.P. van den Bergh, T.A. van Geel, P.P. Geusens, Secondary osteoporosis and metabolic bone disease in patients 50 years and older with osteoporosis or with a recent clinical fracture: a clinical perspective, Curr. Opin. Rheumatol. 26 (2014) 430–439.
[19] A.J. Burghardt, G.J. Kazakia, M. Sode, A.E. de Papp, T.M. Link, S. Majumdar, A longitudinal HR-pQCT study of alendronate treatment in postmenopausal women with low bone density: relations among density, cortical and trabecular microarchitecture, biomechanics, and bone turnover, J. Bone Miner. Res. 25 (2010) 2558–2571.
[20] A.M. Cheung, S. Majumdar, K. Brixen, R. Chapurlat, T. Fuerst, K. Engelke, B. Dardzinski, A. Cabal, N. Verbruggen, S. Ather, E. Rosenberg, A.E. de Papp, Effects of odanacatib on the radius and tibia of postmenopausal women: improvements in bone geometry, microarchitecture, and estimated bone strength, J. Bone Miner. Res. 29 (2014) 1786–1794.
[21] C.E. Kawalilak, J.D. Johnston, W.P. Olszynski, S.A. Kontulainen, Characterizing microarchitectural changes at the distal radius and tibia in postmenopausal women using HR-pQCT, Osteoporos. Int. 25 (2014) 2057–2066.
[22] V.V. Shanbhogue, K. Brixen, S. Hansen, Age- and sex-related changes in bone microarchitecture and estimated strength. A three-year prospective study using HR-pQCT, J. Bone Miner. Res. (2016).
[23] E. Seeman, P.D. Delmas, D.A. Hanley, D. Sellmeyer, A.M. Cheung, E. Shane, A. Kearns, T. Thomas, S.K. Boyd, S. Boutroy, C. Bogado, S. Majumdar, M. Fan, C. Libanati, J. Zanchetta, Microarchitectural deterioration of cortical and trabecular bone: differing effects of denosumab and alendronate, J. Bone Miner. Res. 25 (2010) 1886–1894.
[24] R. Rizzoli, R.D. Chapurlat, J.M. Laroche, M.A. Krieg, T. Thomas, I. Frieling, S. Boutroy, A. Laib, O. Bock, D. Felsenberg, Effects of strontium ranelate and alendronate on bone microstructure in women with osteoporosis. Results of a 2-year study, Osteoporos. Int. 23 (2012) 305–315.
[25] J.N. Tsai, A.V. Uihlein, S.A. Burnett-Bowie, R.M. Neer, Y. Zhu, N. Derrico, H. Lee, M.L. Bouxsein, B.Z. Leder, Comparative effects of teriparatide, denosumab, and combination therapy on peripheral compartmental bone density, microarchitecture, and estimated strength: the DATA-HRpQCT study, J. Bone Miner. Res. 30 (2015) 39–45.
[26] C. Klop, P.M. Welsing, P.J. Elders, J.A. Overbeek, P.C. Souverein, A.M. Burden, H.A. van Onzenoort, H.G. Leufkens, J.W. Bijlsma, F. de Vries, Long-term persistence with anti-osteoporosis drugs after fracture, Osteoporos. Int. 26 (2015) 1831–1840.
[27] J.A. MacNeil, S.K. Boyd, Improved reproducibility of high-resolution peripheral quantitative computed tomography for measurement of bone quality, Med. Eng. Phys. 30 (2008) 792–799.
[28] R. Ellouz, R. Chapurlat, B. van Rietbergen, P. Christen, J.B. Pialat, S. Boutroy, Challenges in longitudinal measurements with HR-pQCT: evaluation of a 3D registration method to improve bone microarchitecture and strength measurement reproducibility, Bone 63 (2014) 147–157.
[29] J.A. MacNeil, S.K. Boyd, Load distribution and the predictive power of morphological indices in the distal radius and tibia by high resolution peripheral quantitative computed tomography, Bone 41 (2007) 129–137.
[30] N. Vilayphiou, S. Boutroy, E. Sornay-Rendu, B. Van Rietbergen, F. Munoz, P.D. Delmas, R. Chapurlat, Finite element analysis performed on radius and tibia HR-pQCT images and fragility fractures at all sites in postmenopausal women, Bone 46 (2010) 1030–1037.
[31] Y. Bala, R. Zebaze, E. Seeman, Role of cortical bone in bone fragility, Curr. Opin. Rheumatol. 27 (2015) 406–413.
[32] N.J. Wachter, P. Augat, G.D. Krischak, M. Mentzel, L. Kinzl, L. Claes, Prediction of cortical bone porosity in vitro by microcomputed tomography, Calcif. Tissue Int. 68 (2001) 38–42.
[33] P. Augat, S. Schorlemmer, The role of cortical bone and its microstructure in bone strength, Age Ageing 35 (Suppl. 2) (2006) ii27–ii31.
[34] C.E. Kawalilak, J.D. Johnston, D.M. Cooper, W.P. Olszynski, S.A. Kontulainen, Role of Endocortical Contouring Methods on Precision of HR-pQCT-Derived Cortical Micro-architecture in Postmenopausal Women and Young Adults, 2016.
[35] B.L. Riggs, L.J. Melton III, R.A. Robb, et al., A population-based study of age and sex differences in bone volumetric density, size, geometry and structure at different skeletal sites, J. Bone Miner. Res. 19 (12) (2004) 1945–1954.